

Effect of α -Platelet Thickness on the Mechanical Properties of Ti-6Al-4V Alloy with Lamellar Microstructure

Y Ren^{1,*}, S M Zhou², Z Y Xue¹, W B Luo³, Y J Ren¹ and Y J Zhang¹

¹ School of energy, power and mechanical engineering, North China Electric Power University, Beijing 102206, PR China

² No. 52 Institute of China Ordnance Industries, Yantai, Shandong 264003, China

³ School of Materials Science and Engineering, University of Science and Technology Beijing, Beijing 100083, PR China

*Email: renyuljz@163.com

Abstract. In this paper, lamellar microstructures with average α -platelet thicknesses ranging from 0.55 μm to 1.98 μm were obtained in Ti-6Al-4V (Ti64) alloy by solution-treated above β -transus temperature and followed cooling through different methods. Then effects of the average thickness of plate-like α phase on the mechanical properties of this alloy were investigated. The results show that the yield stress and/or the flow stress of Ti64 decrease with increased average α -platelet thickness during compression under various strain-rate and temperature conditions. Conversely, the ductility increases with increased average α -platelet thickness. The greater plate thickness facilitates slip and avoids severe pile-up of dislocations in α phase, resulting in the augmentation of the fracture strain as well as decrease of the strength of Ti64. Finally, the variation of yield stress with average α -platelet thickness satisfies Hall-Petch relationship at both quasi-static and dynamic loading strain-rates.

1. Introduction

Ti-6Al-4V alloy (hereafter denoted as Ti64) has been widely used in the aerospace and military industries due to its attractive specific strength, low density and corrosion resistance. Ti64 is a typical two-phase alloy and consists of hexagonal-close-packed (hcp) α and body-centered-cubic (bcc) β phases [1]. This alloy contains about 4 wt.% of the β -stabilizing element vanadium so as to preserve part of β phases at room temperature. Different types of microstructures, such as equiaxed, bimodal or lamellar microstructure, can be obtained in Ti64 through heat treatments conducted under various combinations of temperatures, holding times and cooling-rates [2]. The lamellar (Widmanstätten) microstructure, which can be obtained by means of solid solution at temperatures above beta-transus point in Ti64, is often adopted in the aerospace industry due to its preferable specific strength, fracture toughness (damage tolerance) and creep resistance [3, 4].

Expectedly, the initial microstructural characteristics, such as the morphology, size and volume fraction of equiaxed (primary) α -phase, α -platelet thickness, prior β grain size, etc., will strongly affect the mechanical properties of Ti64 at different temperatures, stress states and strain-rates. Semiatin and Bieler [5] reported that the peak flow stresses of Ti64 with lamellar microstructures during hot compression at 1088–1228 K follow a Hall–Petch dependence on α -platelet thickness. Zhang et al. [6] found that Ti64 with bimodal microstructure has higher fracture strain but lower flow stress than that



with Widmanstätten microstructure at both quasi-static and dynamic strain-rates. After a systematic analysis of the literature data, Wu et al. [7] found that the high cycle fatigue (HCF) strengths of Ti64 decrease in the order of bimodal, lamellar and equiaxed microstructure and microstructure details also has significant influence on the HCF strength of this alloy. Besides, the formability of Ti64 under high temperature conditions depend dramatically on the microstructural characteristics as well [8-10]. However, the effect of microstructure details, such as average α -platelet thickness, on the mechanical properties of Ti64 at broader strain-rates and temperatures has not yet been studied in detail.

In this work, lamellar microstructures with different average α -platelet thicknesses are obtained through heat treatments. Then the effect of the average thickness of the plate-like α -phase on the mechanical properties of this alloy is investigated under various strain-rate and temperature conditions. These findings aid in understanding the deformation behavior of titanium alloys.

2. Materials and experimental procedures

The Ti64 alloy used was a 30 mm-diameter forging bar stocks. The chemical compositions of Ti64 are listed in Table 1. The beta-transus temperature T_β of this alloy determined by differential scanning calorimetry is 1266 K. In order to acquire lamellar microstructures with different α -platelet thicknesses in Ti64, the forging bars were solution-treated at 1286 K, above T_β , for 30 min followed by water quenching (WQ), air cooling (AC) and furnace cooling (FC), respectively [2]. Then these solution-treated materials were annealed at 873 K for 2 h followed by air cooling to relieve the internal stress generated during the cooling process of the solution treatment.

Table 1. Chemical compositions of Ti64 (wt.%).

| Al | V | Fe | O | C | H | N | Ti |
|------|------|------|------|-------|--------|-------|---------|
| 5.82 | 3.84 | 0.16 | 0.08 | 0.024 | 0.0014 | 0.023 | Balance |

The materials were sectioned from the center area of the heat-treated forging bars into several compression cylinders for quasi-static (4 mm in diameter and 8 mm in thickness) and dynamic (4 mm in diameter and 4 mm thick) compression tests. Quasi-static compression tests were performed at both room and elevated (473 K) temperatures under a strain rate of 10^{-3} s^{-1} using an MTS 810 hydraulic servo machine. Tests were continuously conducted until the cylinders fractured. Elevated temperature compression tests were carried out in a high-temperature environmental chamber. Samples were held for 120 s at 473 K before compression. Dynamic compression tests were carried out at room temperature under a strain rate of about 3000 s^{-1} utilizing a split Hopkinson pressure bar (SHPB) apparatus. A more complete description of the SHPB test can be found in Refs. [11, 12].

Optical microscope (OM) and transmission electron microscope (TEM) were employed to determine the microstructural characteristics of the heat-treated forging bars. Specimens for OM studies were prepared by electrochemical polishing in a solution of 95% ethanoic acid + 5% perchloric acid, followed by etching in a solution of 2% HF + 10% HNO₃ + 88% H₂O at room temperature [11]. The metallographical characteristics of Ti64 after heat treatment were examined using a ZEISS Axio Observer A1m optical microscope. TEM analyses were conducted using a JEOL JEM-2100 system at an accelerating voltage of 200 kV. For TEM observations, thin samples with an initial thickness of 0.5 mm were cut from the blocks after OM examinations, reduced to less than 40 μm thick by mechanical means, then punched into several standard 3 mm-diameter TEM discs, and finally thinned by ion milling.

3. Results and discussion

3.1. Microstructural characteristics

Figure 1 shows the optical microstructures of Ti64 after solution-treated and cooled using different methods. The microstructures of the heat-treated Ti64 all show typical lamellar characteristics and consist of acicular or plate-like α phases in equiaxed β matrix. However, the thickness of α -platelet is

significantly distinct in this alloy at different cooling-rates. The mean grain diameter of the equiaxed β matrix is about $698 \pm 33 \mu\text{m}$ and barely varies with decreased cooling-rate, indicating that the prior β grain size is determined more by the solution temperature and the holding time (which are kept constant in this work) rather than the cooling-rate. Besides, some intergranular α with thickness of about $5.7\text{--}16.4 \mu\text{m}$ (indicated by the arrows in Figure 1(c)) can be found in the grain boundaries of the FC material. As shown in Figure 1(a) and (b), when the cooling-rate is very fast (WQ and AC), the thickness of those α -platelets is unable to distinguish accurately due to an insufficient resolution of OM. Hence, more in-depth substructure analyses using TEM must be carried out to further inspect the microstructure details of Ti64 heat-treated at different cooling-rates.

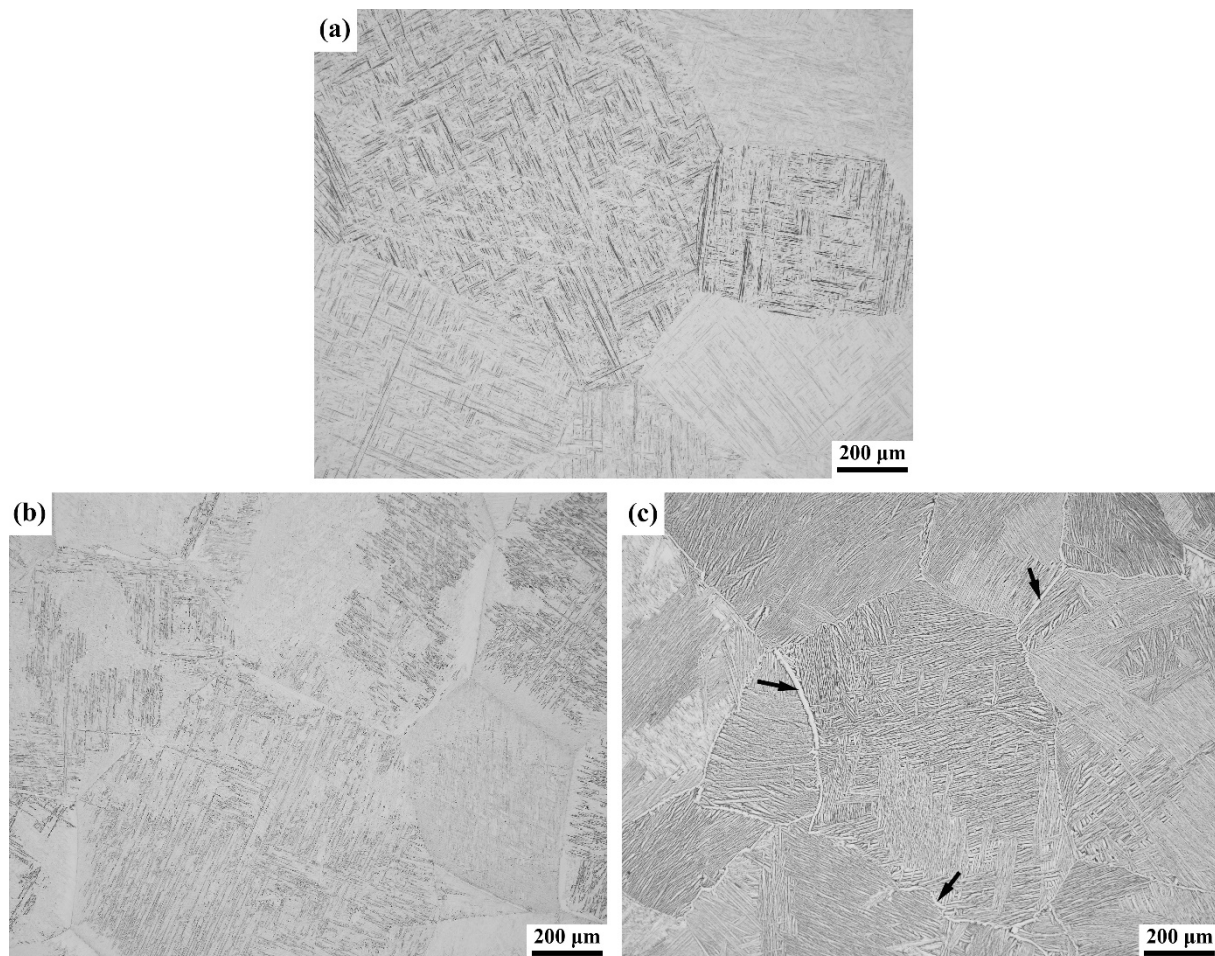


Figure 1. Optical micrographs of Ti64 alloy solution-treated above T_β and then followed by (a) water quenching, (b) air cooling and (c) furnace cooling.

Figure 2 displays the corresponding TEM images of Ti64 with different α -platelet thickness. One can find that the plate-like α phase widens with decreased cooling-rate (from WQ to FC). The distance between two α -platelets increases slightly with decreased cooling-rate. These TEM images also indicate a low dislocation density and the absence of ω phase in alloys before compression testing.

To obtain the precise thickness of α -platelets generated using different cooling methods, statistics were carried out over 20 TEM pictures. The average α -platelet thickness was ascertained using the statistical method for determining average grain size [13]. The result displays that the average α -platelet thickness of Ti64 cooled using WQ, AC and FC methods are $0.55 \pm 0.05 \mu\text{m}$, $0.86 \pm 0.05 \mu\text{m}$ and $1.98 \pm 0.09 \mu\text{m}$, respectively. When the temperature declines below T_β during the cooling process of the

solution treatment, α phase precipitates from the prior β matrix. The precipitation of α platelets involves the nucleation and growth processes of nuclei. The number of nuclei and growth rate are dependent on the composition and the cooling-rate [2]. When the cooling-rate declines, crystal nucleation process is suppressed due to a lower degree of supercooling. Consequently, fewer nuclei make α -platelets have plenty of space to grow, resulting in the formation of wider plates at a lower cooling-rate.

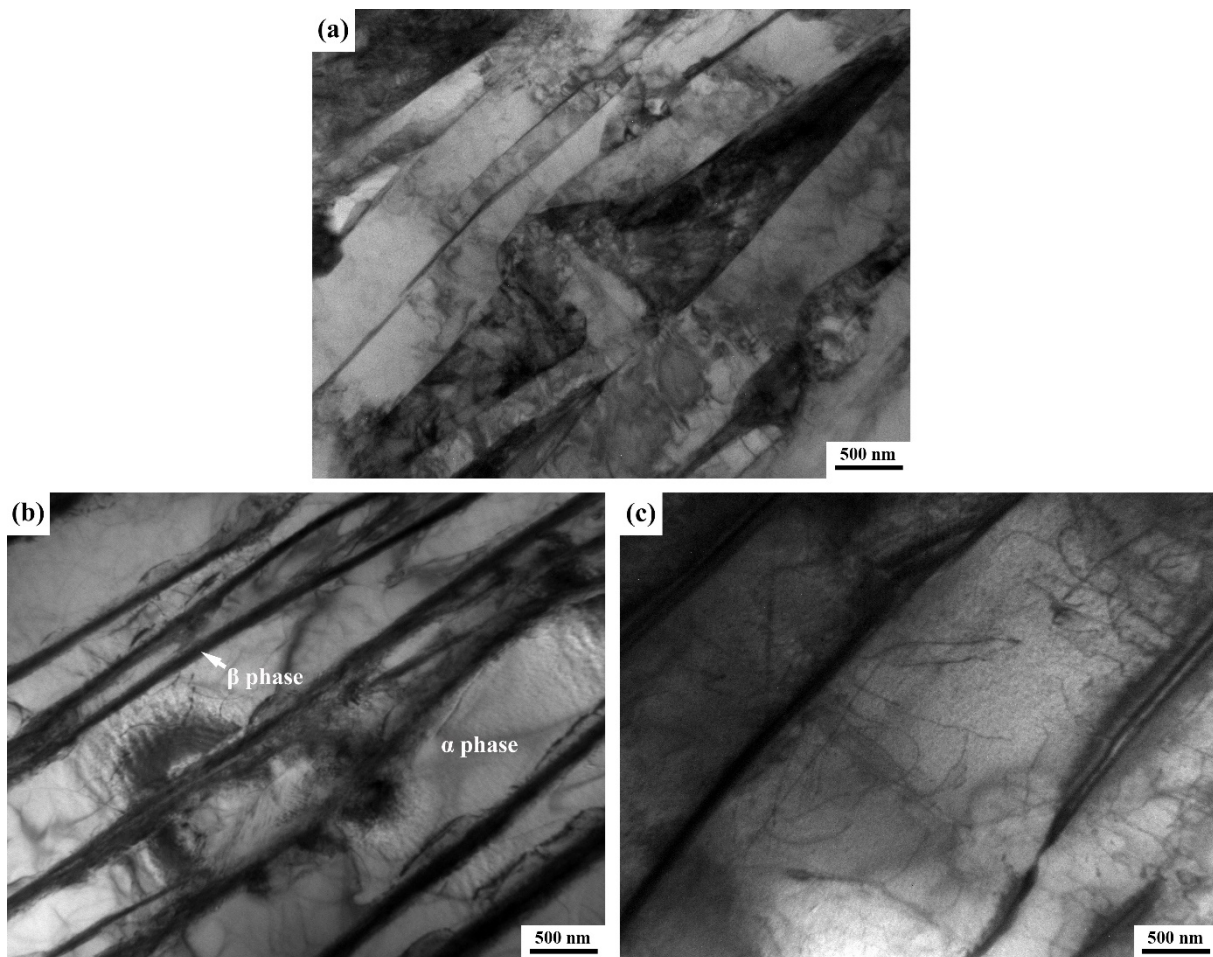


Figure 2. Bright field TEM images of Ti64 alloy solution-treated above T_β and then followed by (a) water quenching, (b) air cooling and (c) furnace cooling.

3.2. Mechanical properties

3.2.1. At quasi-static strain-rate.

Figure 3 presents the compression stress–strain curves and strength variation of Ti64 with different average α -platelet thicknesses at both room temperature and 473 K and at a strain rate of 10^{-3} s^{-1} . At room temperature, as shown in Figure 3(a), the flow stress of Ti64 decreases with increased average α -platelet thickness, although the shape of these curves is similar regardless of the thickness of the plate-like α phase. The strain-hardening rate (SHR) of this alloy hardly changes when the plastic deformation proceeds, implying that the α -platelet thickness has no effect on the SHR of Ti64. On the other hand, the fracture strain increases to some extent (from 0.30 to 0.32) with increased average α -platelet thickness, suggesting the benefit of α -phase broadening on the ductility of Ti64. The fracture strain is defined as the maximum strain that the specimen endures before it fractures during the

compression test. The greater plate thickness facilitates slip and avoids severe pile-up of dislocations in α phase, resulting in the augmentation of the fracture strain as well as decrease of the strength of Ti64.

When the temperature elevates to 473 K (Figure 3(b)), the Ti64 exhibits a certain degree of thermal softening during compression process. Namely, the flow stress of materials decreases with increased plastic strain, i.e. they have a negative SHR during high-temperature compression. The fracture strain also increases with increased average α -platelet thickness. The augmentation of fracture strain is more obvious when the average thickness of plate-like α phase exceeds 1 μm . Figure 3(c) shows the quasi-static compression yield stress as a function of average α -platelet thickness of Ti64 at various temperatures. The yield stress of Ti64 has roughly the same change tendency at both room and elevated temperatures and decreases with increased average α -platelet thickness. All yield stress values at 473 K are about 270 MPa lower than those at room temperature, indicating non-influence of the α -platelet thickness on the decreasing degree of yield stress in Ti64. However, the negative SHR of Ti64 with the α -platelet thickness of 0.86 μm is less evident than the other two (Figure 3(b)), suggesting that AC microstructure has a higher resistance to thermal softening.

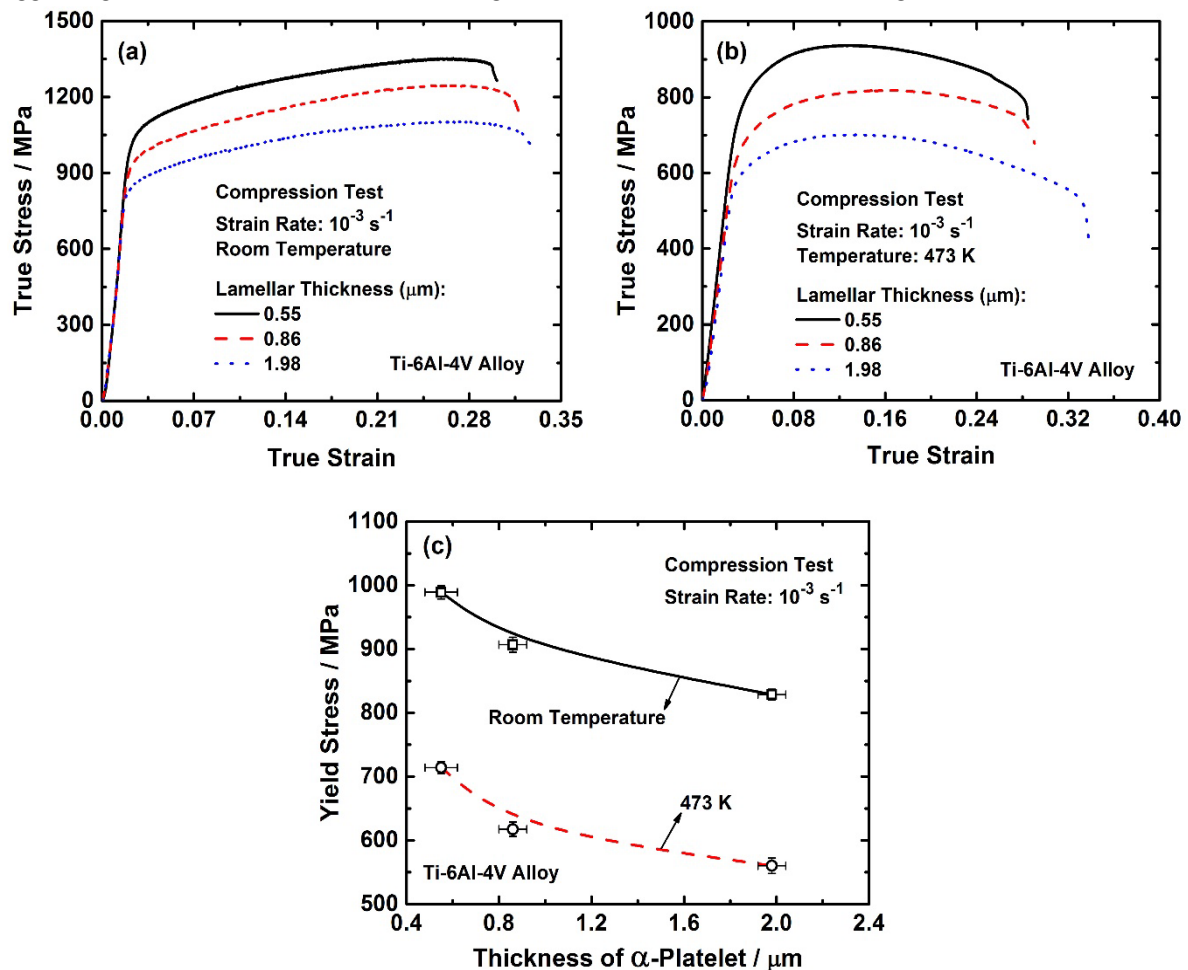


Figure 3. Typical stress–strain curves of Ti64 with different average α -platelet thicknesses quasi-statically compressed at (a) room temperature and (b) 473 K. (c) Yield stress at both room and elevated temperature vs. average α -platelet thickness for Ti64 with lamellar microstructure. Each of the strength values is the average of three measurements.

3.2.2. At dynamic strain-rate.

Figure 4 shows the compression stress–strain curves and strength variation of Ti64 with different average α -platelet thicknesses at room temperature and at a strain rate of about 3000 s^{-1} . Compared with the flow response at quasi-static strain-rate (Figure 3), the α -platelet thickness has a significant impact on the ductility of Ti64 under dynamic strain-rate loading conditions, as shown in Figure 4(a). The fracture strain increases substantially from 0.15 to 0.40 as the average α -platelet thickness increases from $0.55 \mu\text{m}$ to $1.98 \mu\text{m}$. Loading at higher strain-rates leads to more dislocations generated during plastic deformation [12, 14]. So dislocations are more likely to tangle and block at high strain-rate. The greater plate thickness facilitates slip and avoids severe pile-up of dislocations in α phase, resulting in the augmentation of the plastic strain as well as decrease of the strength of Ti64. Besides, the fracture strain of Ti64 with $0.55 \mu\text{m}$ lamellar thickness in dynamic compression test is less than that in quasi-static compression test, while the opposite performance occurs in the material with $1.98 \mu\text{m}$ lamellar thickness. This interesting phenomenon may be related to the dynamic fracture behavior (such as nucleation and propagation of adiabatic shear bands) of Ti64 under high-strain-rate loading conditions. Further in-depth studies have been on the way to verify this conjecture.

The α -platelet thickness also has a more pronounced effect on the SHR and further the thermal softening behavior of Ti64 during dynamic compression process. The SHR gradually reduces with increased average α -platelet thickness, implying a more obvious thermal softening of Ti64 with the wider lamellar microstructure at high strain-rates. The high strain-rate loading process is in an adiabatic state. Thus, the rate of heat generation is greater than the rate of heat loss during deformation at high strain-rates, which increases the temperature of the material. A continuous rise in temperature results in the simultaneous lowering of the flow stress as the strain proceeds [15]. Therefore, greater fracture strain means longer deformation time and more heat accumulation, resulting in a more significant thermal softening effect in Ti64 having a broader lamellar microstructure during dynamic compression. Besides, as shown in Figure 4(b), the yield stress of Ti64 at the strain rate of 3000 s^{-1} also decreases with increased average α -platelet thickness and has a similar change tendency compared to that at quasi-static strain-rate (Figure 3(c)).

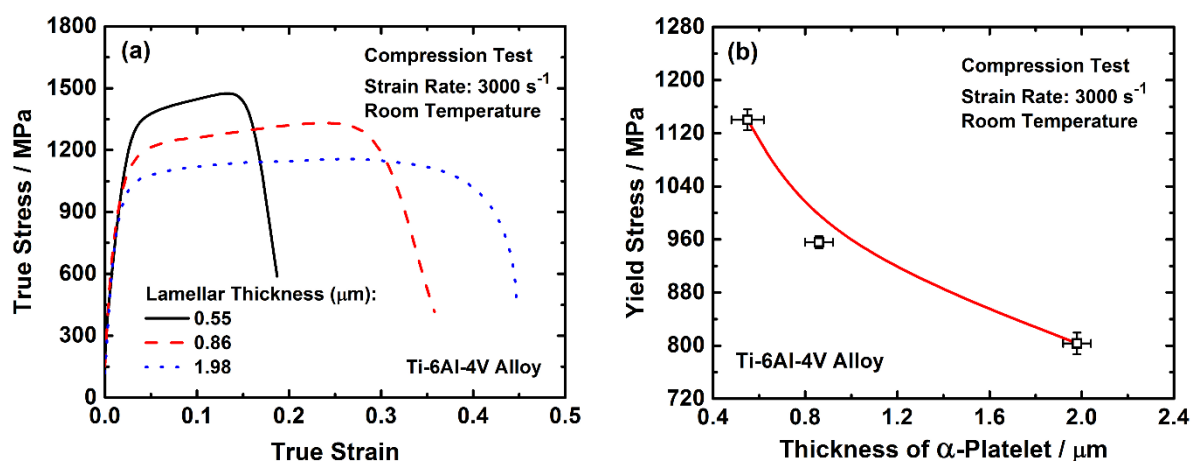


Figure 4. (a) Typical compression stress–strain curves and (b) yield stress vs. average α -platelet thickness for Ti64 with lamellar microstructure at room temperature under a strain rate of 3000 s^{-1} . Each of the strength values is the average of three measurements.

3.3. Hall-Petch behavior

The strengthening behavior generated due to the existence of grain boundaries in most polycrystalline metallic materials can be described through the following formulae known as the Hall–Petch relationship [16]:

$$\sigma = \sigma_0 + k_s \cdot l^{-1/2} \quad (1)$$

where σ is the strength value (yield stress, flow stress or peak stress, etc.), l is the factor quantifying the microstructural scale (grain diameter or α -platelet thickness, etc.), σ_0 and k_s are constants. The Hall–Petch relationship has been successfully applied to explain the deformation behavior of Ti64 at temperatures higher than 1073 K [5, 17]. Hence, this theory is predictably able to be used to describe the deformation behavior of Ti64 under broader strain-rate and temperature conditions. Figure 5 shows the variation of yield stress with the inverse square root of the average α -platelet thickness ($l^{-1/2}$) for Ti64 under different strain-rate and temperature loading conditions. One can find that the yield stress of Ti64 increases linearly with $l^{-1/2}$ in all cases, indicating that the change of yield stress with the average α -platelet thickness of Ti64 obeys the Hall–Petch relationship under a wide range of strain-rates and temperatures. Therefore, linear fitting of these data points according to Equation (1) are carried out. The results are shown in Figure 5 and listed in Table 2.

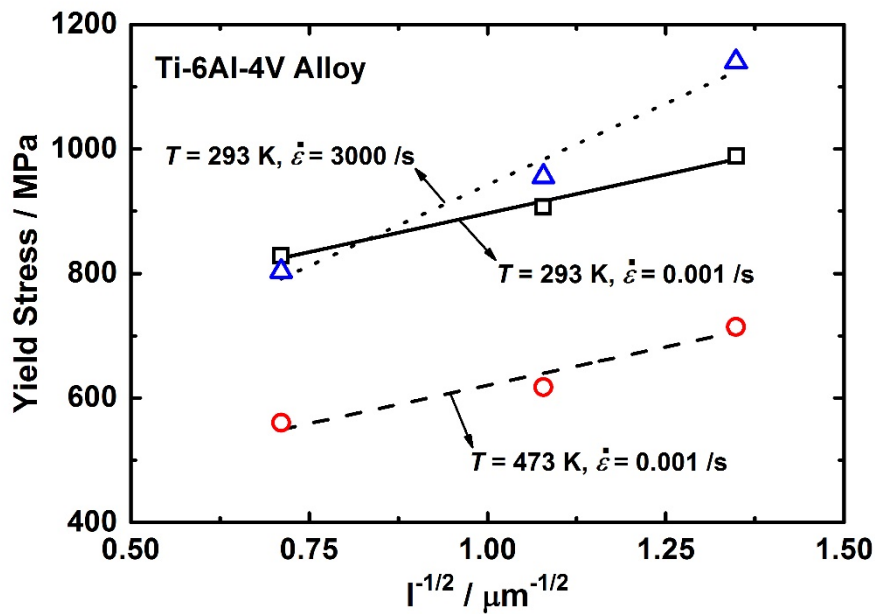


Figure 5. Yield stress vs. the inverse square root of the average α -platelet thickness ($l^{-1/2}$) for Ti64 at various strain-rates and temperatures.

As shown in Table 2, the k_s value significantly increases with increased strain-rate, however, it declines slightly with increased deformation temperature. The constant k_s can be calculated by [18]:

$$k_s = \sqrt{4\sigma^*Gb / \alpha\pi} \quad (2)$$

where σ^* is the barrier strength, G is the shear modulus, b is the burger's vector, and α is a constant. For the same material (Ti64), the value of k_s is only related to σ^* . σ^* value may be a function of strain rate and temperature [5] and increases with increased strain-rate. Hence, at high strain-rate, the augment of yield stress caused by the variation of α -platelet thickness is more obvious in Ti64. The temperature difference in this work is not great, leading to a smaller gap of k_s at quasi-static strain-rate, similar to the behavior of Ti64 at higher temperatures [5]. In addition, the fact that the σ_0 value of Ti64 at dynamic strain-rate is lower than that at quasi-static strain-rate is somewhat surprising. This may be due to the more evident thermal softening in Ti64 with lamellar microstructure (Figure 4(a)).

Table 2. Hall–Petch constants (σ_0 and k_s) based on yield stress data for Ti64 with lamellar microstructures.

| Strain-rate (s ⁻¹) | Temperature (K) | Hall–Petch constants | |
|-----------------------------------|--------------------|----------------------|------------------------------------|
| | | σ_0 (MPa) | k_s (MPa· $\mu\text{m}^{-1/2}$) |
| 0.001 | Room temperature | 647.49 | 249.19 |
| 0.001 | 473 | 374.13 | 246.23 |
| 3000 | Room temperature | 427.47 | 527.88 |

4. Conclusions

Solution treatments with different cooling-rates were carried out on Ti64 to obtain the lamellar microstructures with different average α -platelet thicknesses. Then a series of compression tests were performed on this alloy under various strain-rate and temperature conditions to investigate the effect of the average α -platelet thickness on the mechanical properties of this alloy. The major conclusions are as follows:

- (1) The average α -platelet thicknesses of 0.55 μm , 0.86 μm and 1.98 μm are obtained in Ti64 through solution treatment and subsequently cooled using WQ, AC and FC methods, respectively.
- (2) The yield stress and/or the flow stress of Ti64 decrease with increased average α -platelet thickness during compression under various strain-rate and temperature conditions. Conversely, the ductility increases with increased average α -platelet thickness.
- (3) The greater plate thickness facilitates slip and avoids severe pile-up of dislocations in α phase, resulting in the augmentation of the fracture strain as well as decrease of the strength of Ti64.
- (4) The strengthening effect caused by the α -platelet refinement obeys the Hall–Petch relationship in Ti64 deformed at both quasi-static and dynamic loading strain-rates.

Acknowledgments

This work was supported by the Young Scientists Fund of the National Natural Science Foundation of China (grant number: 51501064).

References

- [1] Joshi V A 2006 *Titanium Alloys: An Atlas of Structures and Fracture Features* (Boca Raton: Taylor & Francis Group) p 9
- [2] Lütjering G and Williams J C 2007 *Titanium (2nd edition)* (Heidelberg: Springer-Verlag Berlin)
- [3] Leyens C and Peters M 2003 *Titanium and Titanium Alloys* (Weinheim: WILEY-VCH Verlag GmbH & Co. KGaA) p 33
- [4] Huo D, Li S and Fan Q 2013 *Rare Metal Mater. Eng.* **42** 0457
- [5] Semiatin S L and Bieler T R 2001 *Acta mater.* **49** 3565
- [6] Zhang J, Tan C, Ren Y, Wang F and Cai H 2011 *Trans. Nonferrous Met. Soc. China* **21** 39
- [7] Wu G Q, Shi C L, Sha W, Sha A X and Jiang H R 2013 *Mater. Des.* **46** 668
- [8] Guan R G, Je Y T, Zhao Z Y and Lee C S 2012 *Mater. Des.* **36** 796
- [9] Wang Y C and Langdon T G 2013 *Mater. Sci. Eng. A* **559** 861
- [10] Fu J, Ding H, Huang Y, Zhang W and Langdon T G 2015 *J. Mater. Res. Tech.* **4** 2
- [11] Liu X Q, Tan C W, Zhang J, Wang F C and Cai H N 2009 *Int. J. Impact Eng.* **36** 1143
- [12] Meyers MA 1994 *Dynamic Behavior of Materials* (New York: John Wiley & Sons, Inc.)
- [13] Bhattacharjee A, Varma V K, Kamat S V, Gogia A K and Bhargava S 2006 *Metall. Mater. Trans.* **37A** 1423
- [14] Asay J R and Shahinpoor M 1992 *High-pressure shock compression of solids* (New York: Springer-Verlag, Inc.)

- [15] Nemat-Nasser S and Guo W G 2003 *Mech. Mater.* **35** 1023
- [16] Armstrong R, Codd I, Douthwaite R M and Petch N J 1962 *Philos. Mag.* **7** 45
- [17] Semiatin S L and Bieler T R 2001 *Metall. Mater. Trans. A* **32A** 1787
- [18] Eshelby J D 1963 *Phys. Status Solidi* **3** 2057